JOURNAL OF SOLID STATE CHEMISTRY **93**, 514–525 (1991)

Synthesis and Crystal Structures of Two Thallium Vanadium Phosphates: $TlVO_2(HPO_4)$ and $Tl_3V_2O_3(VO)(PO_4)_2(HPO_4)$

GUOHE HUAN, JACK W. JOHNSON, ALLAN J. JACOBSON,
EDWARD W. CORCORAN, Jr., AND DAVID P. GOSHORN

Corporate Research Laboratories, Exxon Research and Engineering Company, Annandale, New Jersey 08801

Received January 24, 1991

Two thallium vanadium phosphate compounds have been crystallized hydrothermally and their structures determined by single-crystal X-ray diffraction. The first, a hydrogen phosphate containing only vanadium(V), crystallizes at 450°C and is orthorhombic, space group *Pbca*, with $a = 9.257(2)$ Å, $b = 17.518(4)$ Å, and $c = 6.810(2)$ Å; $V = 1104.4(5)$ Å^3; $Z = 8$; $D_x = 4.610$ g/cm^3; $R = 0.048$; and $R_w = 0.048$ for 564 independent observed reflections with $I \geq 3\sigma(I)$. The structure can be described as chains of corner-sharing distorted square pyramids. Adjacent square pyramids are bridged by the phosphate groups. The chains are linked together by hydrogen bonds to form puckered layers stacked along the *b* axis. The thallium(I) atoms are approximately 7-coordinated by oxygen atoms in sites between the layers. The compound is isostructural with the $MVO_2(HPO_4)$ (M = K, Rb, and NH_4) compounds whose structures were recently determined by powder X-ray diffraction (*1*). The second compound, prepared at 200°C, has the composition $Tl_3V_2O_3(VO)(PO_4)_2(HPO_4)$ and contains both V(V) and V(IV). The structure is orthorhombic, space group *Pnma*, with $a = 7.160(2)$ Å, $b = 13.378(2)$ Å, and $c = 14.422(1)$ Å; $V = 1381.4(7)$ Å^3; $Z = 4$; $D_x = 5.378$ g/cm^3; $R = 0.041$; and $R_w = 0.054$ for 1093 independent observed reflections with $I \geq 3\sigma(I)$. The structure contains vanadium atoms in two independent sites. The vanadium atom V2 is octahedrally coordinated by six oxygen atoms and forms a $-O{=}V{-}O{=}V{-}O-$ chain of composition $VO(PO_4)_2$ along the crystallographic *a* direction. The second vanadium atom (V1) is coordinated by five oxygen atoms in a square pyramidal arrangement and is found as a dimeric unit with composition $V_2O_3(HPO_4)$. The two different units are joined to form the complete vanadium phosphate framework structure by sharing the oxygen atoms of one phosphate group. Bond valence calculations indicate that the vanadium atom in the chain is V^{4+} and that the dimer contains equal amounts of V^{4+} and V^{5+}. The two thallium atoms occupy distorted 8-coordinate sites in the framework. © 1991 Academic Press, Inc.

Introduction

The occurrence of different vanadium coordination geometries and the accessibility of more than one vanadium oxidation state give rise to a rich structural chemistry of vanadium oxide systems. Vanadium–oxygen coordination polyhedra with tetrahedral, octahedral, or distorted octahedral geometries and square pyramidal geometries are typically observed. Larger polyhedral aggregates are formed by condensation of polyhedra through shared oxygen atoms. Coordinated water molecules are often constituents of the vanadium coordination sphere in phases which have been prepared hydrothermally at moderate temperatures. Further structural diversity is obtained when vanadium–oxygen polyhedra are condensed with phosphate building units, such

0022-4596/91 $3.00

as PO_4^{3-}, HPO_4^{2-}, $P_2O_7^{4-}$, and $P_3O_{10}^{5-}$ to form a variety of vanadium phosphates. Alkali metal cations may also be accommodated and a variety of quaternary systems have been characterized. Chain structures are found for $A(VO_2)HPO_4$ (*1, 2*) and layered structures found for $A_2VOP_2O_7$ (*3, 4*) and β-$K_2(VO)_3(P_2O_7)_2$ (*5*) where the V–O–P chains or layers are separated by the A^+ cations. More frequently, three-dimensional frameworks are formed with the A^+ cations located in tunnels in the structure, for example, $LiVOPO_4$ (*6*), $NaV_3P_3O_{12}$ (*7*), $A_2(VO)_3(P_2O_7)_2$ (*8–10*), and AVP_2O_7 (*11–14*).

The present work describes two further members of the A–V–P–O series of compounds where the A^+ cation is thallium. The new phases, $TlVO_2(HPO_4)$ and $Tl_3V_2O_3(VO)(PO_4)_2(HPO_4)$, were synthesized hydrothermally at 450 and 200°C, respectively, and their structures have been determined by single-crystal X-ray diffraction.

Experimental Section

Synthesis

$TlVO_2(HPO_4)$. Thallium oxide (1 mmole; Tl_2O_3, Alfa), vanadium oxide (0.5 mmole; V_2O_3, Alfa), and phosphoric acid (6 mmole; H_3PO_4, Alfa) were introduced into a gold tube. Distilled water (approximately 1 ml) was added to make the total tube filling 60%. The gold tube was welded shut and heated in a cold seal vessel at 450°C and 1 kbar for 2 days. The tube was cooled to room temperature over a period of 4 hr. The yellow plate-like crystals which formed were filtered, washed several times with distilled water, and air-dried (0.25 g, 65.3% yield based on vanadium). Chemical analysis (Galbraith Laboratories) gave 13.42% V, 8.14% P, and 53.15% Tl (calculated for $TlVO_2(HPO_4)$: 13.29% V, 8.08% P, and 53.32% Tl).

$Tl_3V_2O_3(VO)(PO_4)_2(HPO_4)$. Thallium oxide (1 mmole; Tl_2O_3, Alfa), vanadium oxide (1 mmole; V_2O_3, Alfa), and 1.3 g phosphoric acid (85%) were introduced into a 23-ml Teflon-lined steel autoclave. The reaction vessel was filled to ~80% with distilled water, sealed, and maintained at 200°C and autogenous pressure for 4 days. Well-formed black, prismatic single crystals (up to 2 mm in length) were separated by filtration, washed with distilled water, and air-dried (0.56 g, 75.4% yield based on vanadium). Analysis gave 13.92% V, 8.23% P, and 55.17% Tl (calculated for $Tl_3V_2O_3(VO)(PO_4)_2(HPO_4)$; 13.70% V, 8.23% P, and 54.95% Tl).

The vanadium oxidation state in $Tl_3V_2O_3(VO)(PO_4)_2(HPO_4)$ was determined by redox titration. Samples were dissolved in 1 *M* sulfuric acid. A known excess of cerium(IV) ammonium nitrate was added to the vanadium solution to oxidize all of the vanadium ions to the +5 oxidation state. The total vanadium content and the average vanadium oxidation state were then determined potentiometrically by back titration using a standard solution of ferrous ammonium sulfate. The results gave V(IV)/V(V) = 2.0 ± 0.01 and a total vanadium content of 14.27%, in reasonable agreement with the elemental analysis.

A Dupont 1090 thermal analyzer was used to determine the water and hydroxyl contents of both compounds by heating in helium to 1000°C at 10°C min^{-1}. Weight losses were observed at 300°C for $Tl_3V_2O_3(VO)(PO_4)_2(HPO_4)$ and at 320°C for $TlVO_2(HPO_4)$, both of which corresponded to the loss of one-half of a water molecule per formula unit, consistent with condensation of the hydrogen phosphate groups.

X-Ray Diffraction (*15*)

All measurements were made on a Rigaku AFC6R diffractometer with graphite monochromated Mo$K\alpha$ radiation and a 12 kW rotating anode generator. The structures

TABLE I

SUMMARY OF CRYSTAL, DATA COLLECTION, AND REFINEMENT PARAMETERS OF THE STRUCTURES OF $TlVO_2(HPO_4)$ and $Tl_3V_2O_3(VO)(PO_4)_2(HPO_4)$

Crystal data		
Formula	$HTlVPO_6$	$HTl_3V_3P_3O_{16}$
Formula weight	383.29	1115.85
Crystal color, habit	Yellow, plate	Black, prism
Crystal dimensions (mm)	0.20 × 0.20 × 0.05	0.40 × 0.07 × 0.06
Lattice constants		
a(Å)	9.257(2)	7.160(2)
b(Å)	17.518(4)	13.378(2)
c(Å)	6.810(2)	14.422(1)
V(Å^3)	1104.4(5)	1381.4(7)
Space group	*Pbca* (No. 61)	*Pnma* (No. 62)
Z	8	4
Density, calcd. (g cm^{-3})	4.610	5.378
$F(000)$	1336	1940
μ (mm^{-1}), Mo$K\alpha$ (λ = 0.71069 Å)	31.32	37.63
Data collection conditions		
Scan type	$\omega - 2\theta$	ω
Scan speed (°/min, ω)	16 (2 rescans)	16 (2 rescans)
Scan range	$(1.50 + 0.30 \tan \theta)°$	$(0.80 + 0.30 \tan \theta)°$
$2\theta_{max}$	50.0°	50.0°
Total data examined	3334	9734
Unique data examined	970 (R_{int} = 0.120)	1447 (R_{int} = 0.062)
Transmission factors	0.08–1.00	0.67–1.00
Refinement		
R, R_w	0.048, 0.048	0.041, 0.054
Number of observations, $I \geq 3\sigma(I)$	564	1093
Number of variables	53	78
Data/parameter ratio	10.64	14.01
Goodness-of-fit indicator	1.71	2.51

were solved by direct methods and refined by full-matrix least-squares and difference Fourier methods. Details of the data collection and structural refinements are given in Table I. The systematic absences for $TlVO_2(HPO_4)$ uniquely determined the space group as *Pbca*. The systematic absences for $Tl_3V_2O_3(VO)(PO_4)_2(HPO_4)$ indicated that the possible space groups were $Pna2_1$ and *Pnma*. The structure could not be refined acceptably in the noncentrosymmetric group $Pna2_1$ due to near singularities in the normal matrix caused by an apparent mirror plane. Use of the centrosymmetric space group *Pnma* resulted in an acceptable model for the structure if disorder was included at one of the phosphate groups. Four data sets were collected on two different crystals, and all lead to a disordered centrosymmetric model. A complete set ($\pm h$, $\pm k$, $\pm l$) of data was collected on the crystal with the smallest range of transmission factors and was used to determine the final structural model for space group *Pnma*.

Results

Atomic coordinates and thermal parameters for the structures are given in Tables II

TABLE II

ATOMIC COORDINATES AND EQUIVALENT ISOTROPIC DISPLACEMENT COEFFICIENTS (Å^2 × 10^2) FOR $TlVO_2(HPO_4)$

Atom	*x*	*y*	*z*	*B*(eq)
Tl	0.80594(6)	0.10012(5)	0.7253(1)	2.22(5)
V	1.0463(2)	0.2414(2)	1.0167(4)	1.1(1)
P	1.1065(4)	0.0989(3)	1.3012(7)	1.5(2)
O1	1.243(1)	0.0581(8)	1.357(2)	1.7(2)
O2	0.992(1)	0.034(1)	1.267(2)	2.3(2)
O3	1.125(1)	0.1463(9)	1.113(2)	2.4(2)
O4	0.877(1)	0.2269(9)	1.025(2)	2.2(2)
O5	1.100(1)	0.2225(8)	0.784(2)	1.7(2)
O6	1.051(1)	0.3506(9)	0.967(2)	2.0(2)

and III, and important bond distances and angles in Tables IV and V.

Structure Description

TABLE III

ATOMIC COORDINATES AND EQUIVALENT ISOTROPIC DISPLACEMENT COEFFICIENTS (Å^2 × 10^2) FOR $Tl_3V_2O_3(VO)(PO_4)_2(HPO_4)$

Atom	*x*	*y*	*z*	*B*(eq)
Tl1	0.1032(1)	0.01332(5)	0.66338(4)	2.51(3)
Tl2	−0.1270(1)	−0.25	0.50565(6)	2.64(4)
V1	0.1548(3)	0.1232(2)	0.9226(1)	0.88(9)
V2	−0.2512(4)	−0.25	0.7604(2)	0.5(1)
P1	0.0335(4)	−0.1003(2)	0.8805(2)	0.65(5)
O1	−0.463(2)	−0.25	0.8016(8)	0.4(2)
O2	0.209(1)	−0.1447(7)	0.8367(6)	1.2(2)
O3	−0.143(1)	−0.1462(7)	0.8406(6)	1.3(2)
O4	0.045(1)	−0.1194(6)	0.9857(6)	0.9(1)
O5	0.023(1)	0.0121(6)	0.8601(6)	1.0(2)
O6	0.319(1)	0.0624(7)	0.9715(7)	1.5(2)
O7	0.218(2)	0.25	0.957(1)	1.2(2)
P2[a]	0.275(1)	0.25	0.7395(6)	0.2(1)
P3[b]	0.353(2)	0.25	0.7595(7)	0.2
O8	0.571(3)	0.25	0.813(2)	5.7(5)
O9	0.408(2)	0.25	0.658(1)	2.1(3)
O10	0.268(1)	0.1503(7)	0.7981(7)	1.5(2)

[a] Refined occupancy, 0.271(6).

[b] Occupancy, 0.229.

TABLE IV

SELECTED BOND DISTANCES (Å) AND ANGLES (°) FOR $TlVO_2(HPO_4)$

V1–O3	1.93(1)	P1–O1	1.50(1)
V1–O4	1.59(1)	P1–O2	1.57(1)
V1–O5	1.69(1)	P1–O3	1.54(1)
V1–O5	1.99(1)	P1–O6	1.52(1)
V1–O6	1.94(2)	Tl1–O2	3.00(1)
Tl1–O1	2.86(1)	Tl1–O1	2.99(1)
Tl1–O5	2.87(1)	Tl1–O6	3.00(1)
Tl1–O3	2.96(1)	Tl1–O4	3.08(1)
O3–V1–O4	102.9(6)	O1–P1–O2	105.1(8)
O3–V1–O5	92.3(6)	O1–P1–O3	112.1(6)
O3–V1–O5	82.4(5)	O1–P1–O6	111.7(6)
O3–V1–O6	153.9(5)	O2–P1–O3	110.0(7)
O4–V1–O5	106.8(5)	O2–P1–O6	107.7(6)
O4–V1–O5	105.4(5)	O3–P1–O6	110.0(8)
O4–V1–O6	100.8(6)	V1–O3–P1	135.0(8)
O5–V1–O5	147.7(6)	V1–O5–V1	136.2(7)
O5–V1–O6	91.4(6)	V1–O6–P1	135.0(8)
O5–V1–O6	80.7(5)		

$TlVO_2(HPO_4)$. The structure consists of chains of highly distorted corner-sharing VO_5 square pyramids that extend along the *c* axis (see Fig. 1). The V–O distances along the chain (V–O5) alternate between the values 1.69(1) and 1.99(1) Å. The other V–O distances in the base of the pyramid (V–O3 and V–O6) are 1.93(1) and 1.94(2) Å, respectively. Both the O3 and O6 oxygen atoms are shared with phosphate groups. The fifth oxygen in the distorted square pyramid (O4) is perpendicular to the chains and its distance to vanadium (1.59(1) Å) is the shortest, indicating a multiple-bond character. Each phosphate group bridges two vanadium atom square pyramids by sharing the atoms O3 and O6. These oxygen atoms are *trans* to each other within a square pyramid and consequently the phosphate tetrahedra are on either side of the chain (see Fig. 1). Each phosphate tetrahedron has two oxygen atoms (O1 and O2) which are not coordinated to vanadium atoms and therefore do not form part of the chain connectivity. The average P–O distance is 1.53(1) Å, but the distance from the phosphorus atom to the

TABLE V

SELECTED BOND DISTANCES (Å) AND ANGLES (°) FOR $Tl_3O_2O_3(VO)(PO_4)_2(HPO_4)$

V1–O4	1.950(9)	V2–O1	1.63(1)
V1–O5	1.978(9)	V2–O1	2.25(1)
V1–O6	1.59(1)	V2–O2	2.007(9) [×2]
V1–O7	1.826(5)	V2–O3	1.97(1) [×2]
V1–O10	2.00(1)		
		P2–O8	1.64(2)
P1–O2	1.528(9)	P2–O9	1.51(2)
P1–O3	1.518(9)	P2–O10	1.58(1) [×2]
P1–O4	1.540(9)	P3–O8	1.74(3)
P1–O5	1.534(9)	P3–O9	1.52(2)
		P3–O10	1.57(1) [×2]
Tl1–O3	2.805(9)		
Tl1–O6	2.89(1)	Tl2–O8	2.81(1)
Tl1–O5	2.896(9)	Tl2–O2	2.920(9) [×2]
Tl1–O10	2.919(9)	Tl2–O4	2.928(9) [×2]
Tl1–O6	3.00(1)	Tl2–O7	3.01(1)
Tl1–O5	3.024(9)	Tl2–O1	3.02(1)
Tl1–O10	3.07(1)	Tl2–O9	3.10(1)
Tl1–O2	3.193(3)		
O4–V1–O5	86.5(4)	O2–P1–O3	111.8(5)
O4–V1–O6	103.1(4)	O2–P1–O4	107.3(5)
O4–V1–O7	91.3(5)	O2–P1–O5	110.1(5)
O4–V1–O10	155.4(4)	O3–P1–O4	110.6(5)
O5–V1–O6	99.8(4)	O3–P1–O5	106.4(5)
O5–V1–O7	160.3(4)	O4–P1–O5	110.8(5)
O5–V1–O10	85.5(4)	O8–P2–O9	102(1)
O6–V1–O7	99.8(5)	O8–P2–O10	102.5(7)
O6–V1–O10	101.1(5)	O9–P2–O10	115.9(5)
O7–V1–O10	88.6(5)	O10–P2–O10	115.2(9)
O1–V2–O1	178.0(3)	O8–P3–O9	101(1)
O1–V2–O2	97.1(4)	O8–P3–O10	101.1(7)
O1–V2–O3	98.8(4)	O9–P3–O10	116.4(6)
O1–V2–O2	81.5(4)	O10–P3–O10	116.6(9)
O1–V2–O3	82.6(3)	V2–O1–V2	135.2(6)
O2–V2–O2	89.1(5)		
O2–V2–O3	164.1(4)		
O2–V2–O3	88.3(4)		
O3–V2–O3	89.8(6)		

oxygen atom O1 is shorter (1.50(1) Å) and the distance from the phosphorus atom to the oxygen atom O2 (1.57(2) Å) is longer. These distances from the phosphorus atom to the oxygen atoms that are not shared with vanadium show that the O2 atom is part of a hydroxyl group. The O1–O2 distance between adjacent chains is 2.49(1) Å, indicating the presence of hydrogen bonding which acts to join the chains together along *a* to form layers in the *ac* plane, as indicated in Fig. 2. The V=O groups are oriented in opposite directions in adjacent layers.

The thallium atoms occupy highly distorted sites between the layers (Fig. 1) and are 7-coordinated by oxygen atoms from three adjacent chains. Each thallium atom is coordinated to the phosphate oxygen atoms

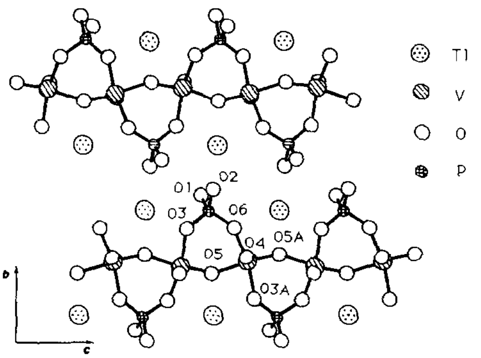

FIG. 1. The structure of $TlVO_2(HPO_4)$ projected into the *bc* plane, showing the chains of VO_5 square pyramids, the bidentate phosphate groups, and the interchain thallium positions.

O1 and O2 in one layer. In the adjacent layer, each thallium atom is coordinated to one phosphate oxygen atom (O1) and to four oxygen atoms (O3, O4, O5, and O6) which are also coordinated to vanadium atoms. In addition, three further contacts are present at longer distances (O6, 3.27 Å; O4, 3.39 Å; O5, 3.49 Å). Bond valence calculations (Table VI) indicate that the vanadium is present as V(V) as anticipated from the color and that the thallium is Tl(I).

$Tl_3V_2O_3(VO)(PO_4)_2(HPO_4)$. The structure contains vanadium atoms in two independent sites. The vanadium atom V2 is coordinated by six oxygen atoms to form a distorted octahedron with approximate C_{4v} symmetry. The V2 octahedra form a chain of stoichiometry, $VO(PO_4)_2$, along the crystallographic *a* direction by sharing the O1 oxygen atoms at *trans* corners. The vana-

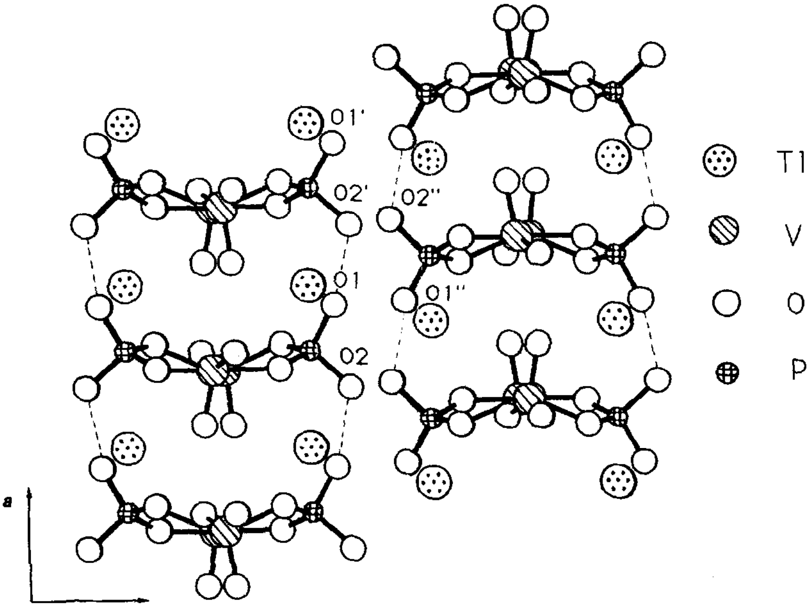

FIG. 2. The structure of $TlVO_2(HPO_4)$ projected into the *ab* plane, showing the chains of VO_5 square pyramids edge on and the vanadyl oxygen atoms approximately perpendicular to the chain direction. Hydrogen bonds (dotted lines) are formed between O1 and O2 to link the chains together along *a* to form layers.

TABLE VI

BOND VALENCES FOR $TlVO_2(HPO_4)$ AND $Tl_3V_2O_3(VO)(PO_4)_2(HPO_4)$

	Distance (Å)	Bond valence
$TlVO_2(HPO_4)$		
V		
O3	1.93(1)	0.645
O4	1.59(1)	1.872
O5	1.69(1)	1.368
O6	1.94(1)	0.625
O5′	1.99(1)	0.534
		$\Sigma_s = 5.044$
P		
O1	1.50(1)	1.396
O2	1.57(2)	1.149
O3	1.54(1)	1.249
O6	1.52(1)	1.320
		$\Sigma_s = 5.114$
$Tl_3V_2O_3(VO)(PO_4)_2(HPO_4)$		
V1		
O4	1.950(9)	0.606
O5	1.978(9)	0.555
O6	1.59(1)	1.872
O7	1.826(5)	0.893
O9	2.71(1)	0.056
O10	2.00(1)	0.506
		$\Sigma_s = 4.488$
V2		
O1	1.63(1)	1.651
O1′	2.25(1)	0.236
O2	2.007(9)	0.506
O2′	2.007(9)	0.506
O3	1.97(1)	0.569
O3′	1.97(1)	0.569
		$\Sigma_s = 4.038$

Note. Bond valences were calculated using $s = \exp[-(R - R_0)/B]$ and the parameters V: $R_0 = 1.79$ Å, $B = 0.319$; P: $R_0 = 1.62$ Å, $B = 0.36$; and Tl: $R_0 = 1.94$ Å, $B = 0.50$ (Ref. (*24*)).

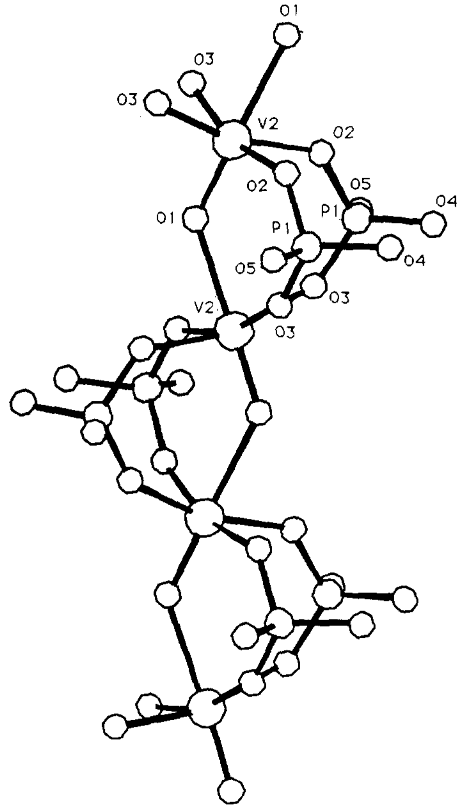

FIG. 3. The V^{4+} chain in $Tl_3V_2O_3(VO)(PO_4)_2(HPO_4)$ formed by V2 octahedra and P1 tetrahedra that extends along the *a* direction.

dium–oxygen distances along the chain alternate between short (1.63(1) Å) and long (2.25(1) Å) and the chain can be represented as –O═V–O═V–O–. The phosphate groups containing the P1 atom connect adjacent V2 atoms in the chain by sharing the oxygen atoms O2 and O3 to give the overall chain geometry shown in Fig. 3. The second vanadium atom (V1) is coordinated by five oxygen atoms in a square pyramidal arrangement and is found as a dimeric unit along with the disordered P2 phosphate group. The V1 dimer straddles the mirror plane and is connected through a bridging oxide ion (O7) and the chelating disordered phosphate group (P2, P3). Atoms P2 (and P3), O7, O8, and O9 reside on the mirror plane. The V1 dimer unit is shown in Fig. 4 with only P2 of the P2, P3 pair represented for clarity. The oxygen atom O9 is located above the square face of the V1 pyramid at a distance of 2.71(1) Å from the vanadium atom occupying what would be the sixth coordination site of the V1 octahedron if it were closer. Bond valence calculations

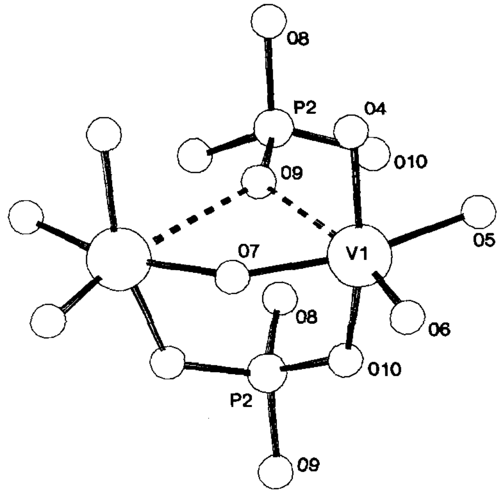

FIG. 4. The dimeric $V_2O_3^{3+}$ unit in $Tl_3V_2O_3(VO)(PO_4)_2(HPO_4)$ formed by the V1 square pyramids and the P2 tetrahedra.

indicate a V1–O9 bond order of only 0.056, justifying the description of V1 as 5-coordinated. The disorder arises in the location of the phosphorus atom. The P3 atom occupies the tetrahedral hole formed by the O9 and two O10 atoms of the P2 tetrahedron together with the O8 atom below them. Refinement indicated approximately equal occupancies (0.271, 0.229) for P2 and P3. Bond valence calculations indicate that O8 is the oxygen atom of the hydroxyl group. The $V_2O_3(HPO_4)$ units are linked together in the *a* direction by hydrogen bonding from O8 to O9 (d_{O8-O9} = 2.52(3) Å). Of course, this hydrogen bonding distance between two P2 tetrahedra corresponds to the tetrahedral edge in the P3 tetrahedron (not shown). The bond distances about P2, P3 and O8 are inaccurate because of the disorder. The complete vanadium phosphate framework structure is shown viewed down **a** in Fig. 5. The linear chains of composition $VO(PO_4)_2$ are located at approximately $(x, \frac{1}{4}, \frac{1}{4})$ in the unit cell and the $V_2O_3(HPO_4)$ units are at $(x, \frac{1}{4}, \frac{3}{4})$. The two different units are joined by sharing O4 and O5 atoms of the P1 phosphate groups. Bond valence calculations indicate that V2 is V^{4+} and that the V1 dimer contains equal amounts of V^{4+} and V^{5+} (see Table VI). The two thallium atoms occupy distorted 8-coordinate sites in the framework. Tl(1) is coordinated by O10 × 2, O5 × 2, O6 × 2, O3, and O8; and Tl(2) is coordinated by O4 × 2, O2 × 2, O1, O7, O8, and O9.

Magnetic Properties

The magnetic susceptibility of $Tl_3V_2O_3(VO)(PO_4)_2(HPO_4)$ was measured as a function of temperature between 8 and 350 K using a George Associates Faraday magnetometer with an applied magnetic field of 6.2 kG and is displayed in Fig. 6. The data were fitted in the temperature range 50–350 K using the Curie–Weiss formula: $\chi = \chi_0 + C/(T - \theta)$ with $\chi_0 = -9.98 \times 10^{-8}$ g cm^{-3}, $C = 6.40 \times 10^{-4}$ g cm^{-3} K, and $\theta = 1.0$ K. The μ_{eff} value calculated from the Curie constant is 1.69 BM per V^{4+} atom if two of the three vanadium atoms in the formula unit are assumed to be tetravalent, consistent with the bond valence calculations.

Discussion

The compounds $AHVPO_6$(A = NH_4^+, K^+, Rb^+, and Cs^+) were first reported by Preuss and Schug (*16*) and subsequently further characterized (*2*). The structures of the NH_4^+, K^+, and Rb^+ compounds were recently determined by Amoros *et al.* (*1*) using powder samples due to difficulty in obtaining single crystals. The Cs^+ phase could not be characterized in detail because of disorder associated with the layer stacking, but it is thought to be isostructural. In this paper, the previously unreported thallium analogue has been prepared hydrothermally in single-crystal form and its structure has been determined. The Tl phase is isostructural with the other members of the series and the structure confirms that the correct

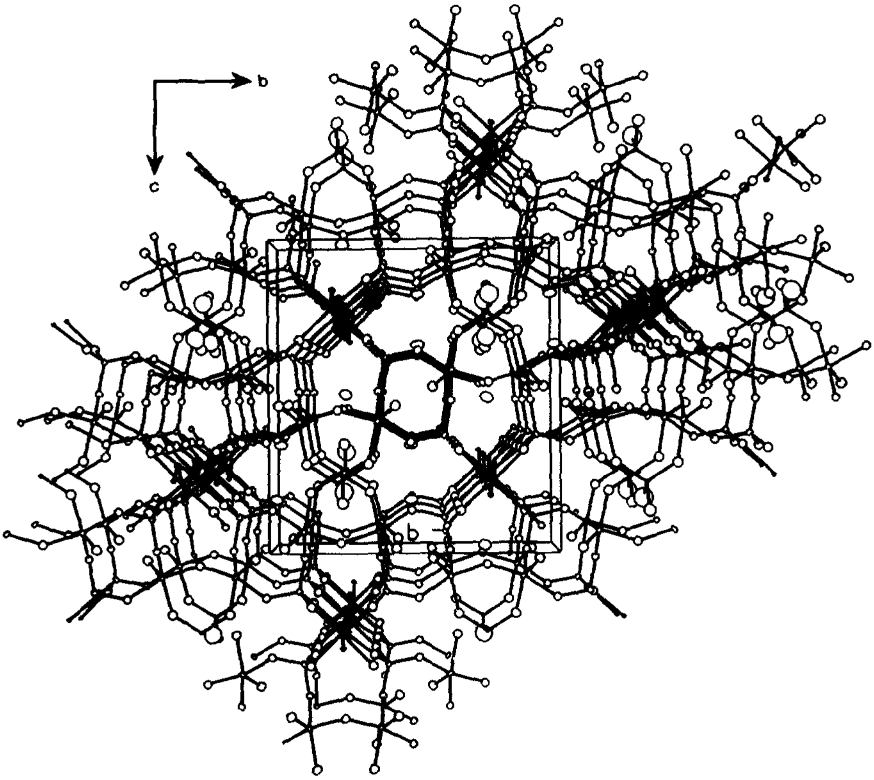

FIG. 5. The unit cell of $Tl_3V_2O_3(VO)(PO_4)_2(HPO_4)$ viewed down the *a* axis. The $VO(PO_4)_2$ chains are located at approximately x, $\frac{1}{4}$, $\frac{1}{4}$ and the $V_2O_3(HPO_4)$ units are at approximately x, $\frac{1}{4}$, $\frac{3}{4}$.

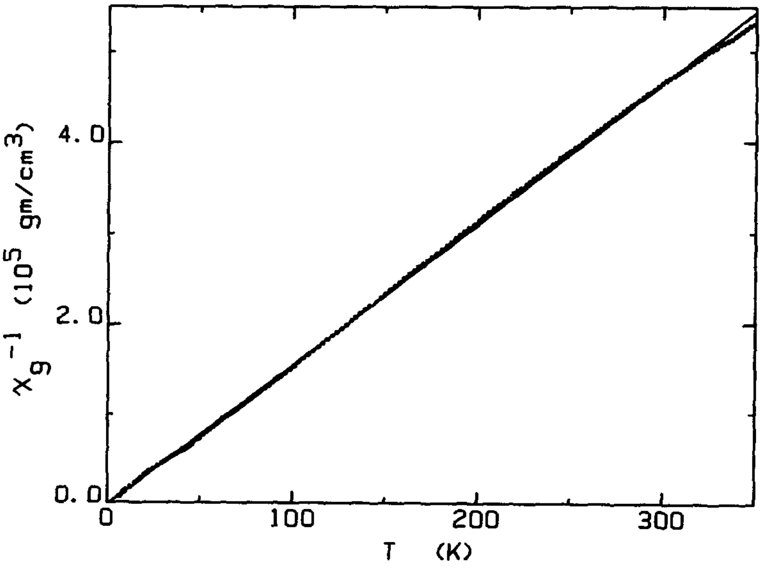

FIG. 6. Inverse magnetic susceptibility of $Tl_3V_2O_3(VO)(PO_4)_2(HPO_4)$ plotted vs temperature. The solid line is a fit of the data to the Curie–Weiss law from 50–350 K.

formulation of the compounds is $AVO_2(HPO_4)$ and not $A(VOOH)PO_4$ (2). In the previous structural study the hydrogen atoms were not located, although it was suggested that they were likely to be near the uncoordinated oxygen atoms of the phosphate groups. The bond valences for O2 and O1 are calculated from the phosphorus oxygen bond lengths to be 1.20 and 1.55, compared with the calculated values of 1.91–2.00 for the other framework oxygen atoms in the structure. This locates the hydrogen atoms as bonded to O2 and hydrogen bonded to O1. The hydrogen bonded network connects adjacent chains together to form layers in the *ac* plane as described above. The thallium atoms occupy interlayer sites coordinated by oxygen atoms.

The changes in cell dimensions for the series of compounds $AVO_2(HPO_4)(A^+ = K^+, Tl^+, Rb^+$, and $Cs^+)$ correlate with the size of the interlayer cation (*23*). The effect is least pronounced for the *c* axis, the length of which is determined by the PO_4 bridged –O═V–O═V– chain. (The unit cells described in Amoros *et al.* (*1*), and Pulvin *et al.* (*2*) are related to the description used here by the transformations **cab** and **acb**, respectively.) Larger dimensional changes found in the *a* and *b* axis lengths are plotted in Fig. 7. Changes in the *a* axis length affect the hydrogen bonding network which connects the chains into layers and are consequently smaller than changes in *b* which effect only the interlayer separation *b*/2.

The $Tl_3V_2O_3(VO)(PO_4)_2(HPO_4)$ structure is a new structure type, although it contains several structural elements in common with other alkali metal vanadium(IV) phosphate phases. A survey of the simple and alkali metal containing vanadium(IV) phosphates and hydrogen phosphates is given in Table VII. A characteristic feature of all of these compounds is that the vanadium coordination by oxygen is either distorted octahedral or square pyramidal. The vanadium atom has one short bond to oxygen, typically in the range 1.56–1.75 Å, characteristic of substantial multiple bonding as indicated by the corresponding estimated bond orders of 2.0 to 1.1. In the simplest hydrated phosphate or hydrogen phosphate structures, the vanadium oxygen polyhedra are found as isolated units connected by oxygen atoms shared with phosphate groups. In the anhydrous phosphate and hydrogen phosphate structures the units condense to form –O═V–O═V–O– chains of various kinds depending on the phosphate connectivity. Three different examples are observed in the known structures. In the simplest case, there are no bridging phosphate groups and the –O═V–O═V–O– chain is linear. A single phosphate bridging between adjacent octahedra in the chain results in a staggered chain with a V–O–V angle of 135°–145°, depending on the degree of twist about the chain axis. A larger V–O–V angle of 165° is observed when the chain is bridged by a pyrophosphate group. The various known examples of these different chain arrangements are summarized in Table VII. The $Tl_3V_2O_3(VO)(PO_4)_2(HPO_4)$ compound described in this paper is an example of a phosphate-bridged chain structure with a 135° V–O–V angle. When alkali metals are intro-

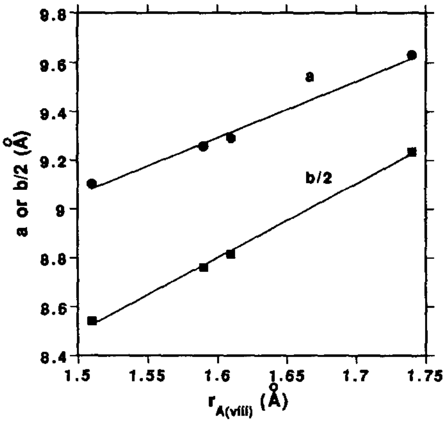

FIG. 7. Variation of the cell constants of $AVO_2(HPO_4)$ phases with *A* cation size.

TABLE VII

SELECTED STRUCTURAL INFORMATION FOR SOME VANADIUM(IV) PHOSPHATES AND HYDROGEN PHOSPHATES

Dimers or isolated units	O=V–O distances (Å)[a]	Structure		Reference
$VO(HPO_4) \cdot 1/2H_2O$	1.600, 2.382	Dimers	Layer	(18)
$VO(HPO_4) \cdot 4H_2O$	1.604, 2.287	Isolated	Chain	(18)
α-$VO(HPO_4) \cdot 2H_2O$	1.601, 2.347	Isolated	Layer	(19)
$K_2VOP_2O_7$	1.604	Isolated	Layer	(3)
$Rb_2VOP_2O_7$	1.597	Isolated	Layer	(4)
$Cs_2VOP_2O_7$	1.592	Isolated	Layer	(4)
$K_2(VO)_3(P_2O_7)_2$	1.59 1.61, 2.46	Dimers	3D	(10)
$Rb_2(VO)_3(P_2O_7)_2$	1.595 1.581, 2.480	Dimers	3D	(8)
$Cs_2(VO)_3(P_2O_7)_2$	1.589 1.580, 2.692	Dimers	3D	(9)
$Tl_3V_2O_3(VO)(PO_4)_2(HPO_4)$	1.59, 2.71	Dimers	3D	This work
β-$K_2(VO)_3(P_2O_7)_2$	1.618	Isolated	Layer	(5)
Linear chains	**O=V–O distances (Å)[a]**	**V–O–V (°)**	**Structure**	**Reference**
$(VO)_2P_2O_7$	1.73, 2.21 1.70, 2.17 1.53, 2.34 1.55, 2.37	180	Layer	(20)
$VOSi(PO_4)_2$	1.59, 2.49	180	Layer	(21, 22)
β-$K_2(VO)_3(P_2O_7)_2$	1.642, 2.521	180	Layer	(5)
$LiVOPO_4$	1.626, 2.240	139.1, 136.6	3D	(6)
$Tl_3V_2O_3(VO)(PO_4)_2(HPO_4)$	1.63, 2.25	135.2	3D	This work
$K_2(VO)_3(P_2O_7)_2$	1.67, 2.03	165	3D	(10)
$Rb_2(VO)_3(P_2O_7)_2$	1.617, 2.063	162.0, 164.5	3D	(8)
$Cs_2(VO)_3(P_2O_7)_2$	1.615, 2.072	167.3, 166.6	3D	(9)

[a] When two distances are given, the vanadium atom is 6-coordinated by oxygen in a distorted octahedron; when one distance is given the vanadium atom is 5-coordinated in a square pyramid.

duced into the vanadium phosphates the structures become more elaborate than those observed in the simple ternary compounds. Large alkali metals are accommodated by forming layer structures as found for the $A_2VOP_2O_7$ (3, 4) compounds and for β-$K_2(VO)_3(P_2O_7)_2$ (5) or alternatively by introducing isolated units or dimers in combination with chains as observed in the $A_2(VO)_3(P_2O_7)_2$ (8–10) compounds and in the structure of $Tl_3V_2O_3(VO)(PO_4)_2(HPO_4)$. A combination of isolated units and chains is also found in the recently reported mixed valence compound $RbV_3P_4O_{17.14}$ (17). The structure of this phase though disordered contains both an infinite and a four-membered chain. Surprisingly, no alternation of bond lengths along the infinite octahedral V(IV) chain is observed, presumably due to the disorder.

Hydrothermal synthesis provides a route to new phases in the form of single crystals suitable for structure determination. The high partial pressure of water present during synthesis results in the incorporation of hydrogen phosphate groups. Consequently, hydrogen bonding plays a significant role in determining the overall structural connectivity. The two structures described above both contain important hydrogen bonded networks. The chains of $TlVO_2(HPO_4)$ are held together to form layers in the *ab* plane by hydrogen bonds, while in $Tl_3V_2O_3(VO)(PO_4)_2(HPO_4)$ hydrogen bonding links the $V_2O_3(HPO_4)$ units together in the *a* direction.

References

1. P. Amoros, D. Beltran-Porter, A. Le Bail, G. Ferey, and G. Villeneuve, *Eur. J. Solid State Inorg. Chem.* **25,** 599 (1988).
2. S. Pulvin, E. Bordes, M. Ronis, and P. Courtine, *J. Chem. Res. Synop.*, 29 (1981); *J. Chem. Res. Miniprint*, 362 (1981).
3. Y. E. Gorbunova, S. A. Linde, A. V. Lavrov, and I. V. Tananaev, *Dokl. Akad. Nauk SSSR* **250,** 350 (1980).
4. K. H. Lii and S. L. Wang, *J. Solid State Chem.* **82,** 239 (1989).
5. K. H. Lii, H. J. Tsai, and S. L. Wang, *J. Solid State Chem.* **87,** 396 (1990).
6. A. V. Lavrov, *Dokl. Akad. Nauk SSSR* **266,** 343 (1982).
7. N. Kinomura, M. Matsui, N. Kumada, and F. Muto, *J. Solid State Chem.* **79,** 232 (1989).
8. K. H. Lii, Y. P. Wang, C. Y. Cheng, S. L. Wang, and H. C. Ku, *J. Chin. Chem. Soc.* **37,** 141 (1990).
9. K. H. Lii, Y. P. Wang, and S. L. Wang, *J. Solid State Chem.* **80,** 127 (1989).
10. A. Leclaire, H. Chahboun, D. Groult, and B. Raveau, *J. Solid State Chem.* **77,** 170 (1988).
11. U. Florke, *Z. Kristallogr.* **191,** 137 (1990).
12. K. H. Lii, Y. P. Wang, Y. B. Chen, and S. L. Wang, *J. Solid State Chem.* **86,** 143 (1990).
13. Y. P. Wang and K. H. Lii, *Acta Crystallogr. Sect. C* **45,** 1210 (1989).
14. Y. P. Wang, K. H. Lii, and S. L. Wang, *Acta Crystallogr. Sect. C* **45,** 1417 (1989).
15. Molecular Structure Corp., The Woodlands, TX.
16. F. Preuss and H. Schug, *Z. Naturforsch. B* **30,** 334 (1975).
17. K. H. Lii and C. S. Lee, *Inorg. Chem.* **29,** 3298 (1990).
18. M. E. Leonowicz, J. W. Johnson, J. F. Brody, H. F. Shannon, Jr., and J. M. Newsam, *J. Solid State Chem.* **56,** 370 (1985).
19. A. Le Bail, G. Ferey, P. Amoros, and D. Beltran-Porter, *Eur. J. Solid State Inorg. Chem.* **26,** 419 (1989).
20. Y. E. Gorbunova and S. A. Linde, *Sov. Phys. Dokl.* **24,** 138 (1979).
21. N. Middlemiss and C. Calvo, *Acta Crystallogr. Sect. B* **32,** 2896 (1976).
22. C. E. Rice, W. R. Robinson, and B. C. Tofield, *Inorg. Chem.* **15,** 345 (1976).
23. R. D. Shannon, *Acta Crystallogr. Sect. A* **32,** 751 (1976).
24. I. D. Brown, *in* "Structure and Bonding in Crystals" (M. O'Keefe and A. Navrotsky, Eds.), Vol. II, Academic Press, New York (1981).